Improved fast electron transport through the use of foam guides

R. A. B. Alraddadi,[1] A. P. L. Robinson,[2] and N. C. Woolsey[3]

[1)] *Department of Physics and Astronomy, College of Science, King Saud University, P. O. Box 2455, Riyadh, Saudi Arabia*

[2)] *Central Laser Facility, STFC Rutherford-Appleton Laboratory, Didcot, OX11 0QX, United Kingdom*

[3)] *York Plasma Institute, University of York, York YO10 5DD, United Kingdom*

The observation that ultra-intense lasers acting on solid targets results in high absorption is exciting for applications, but the high divergence of the fast electrons carrying this energy remains a key limitation for developing many concepts. We show using three-dimensional simulations how low-density foam filled resistive guide targets lead to fast electron collimation over extended distance. Our analysis shows that long mean free paths of the resistive currents in a foam leads to good collimation. We introduce the use of composite concepts, or hybrid resistive guide target, that couples the advantage of high laser absorption and strong collimation of solid-density guides, with the low-scattering properties and long transport distances of foam-filled guides.

I. INTRODUCTION

Controlling laser-driven fast (relativistic) electron divergence, i.e. collimation, is a significant challenge in the field of ultraintense laser-plasma interactions. Experimental measurements[1,2] indicate that the generated fast electrons beam spray outwards with a large divergence angle. This has been attributed to a number of factors ranging from the scattering with ions and background electrons[3,4] through to the influence of the magnetic field near the critical surface[4,5]. Achieving collimation of the fast electron beam is seen as critically important for the success of certain applications, such as fast ignition (FI) approach[6] to inertial confinement fusion[7]. In the FI scheme, the large divergence of the fast electron beam reduces the coupling efficiency as the stand-off distance is several times the size of the centre of the compressed fuel and fast electron source[4].

Self-collimation[8] can be sufficient when the resistive magnetic field is able to deflect a fast electron through characteristic divergence half-angle in the same distance that it takes the beam radius to double. However experimental results indicate that the intrinsic fast electron divergence is so large[2] that self-collimation is highly unlikely in most situations. This has led researchers to consider schemes that could induce collimation. A number of schemes have been proposed, for instance, magnetising targets via external magnetic field[9,10], the use of doped foam target with high Z material[11] or of compressed target[12], double laser pulse approach[13–15] and resistive guiding concept[16]. The latter has shown an excellent collimation and confinement of the fast electron beam within the guide[17,18] and proposed to be used as tool to drive hydrodynamics[19]. Recent work in resistive guiding concept focused on reinforcing the resistive magnetic collimation[20], improving the large radius wire-guide heating with depth[21,22] and producing a more collimated beam for propagation through homogeneous material[23].

In this work, we propose a new variation in the class of laser-generated fast electron guiding schemes; resistive guide target is made from a pure foam or of combining both foam and solid materials. We called it a hybrid resistive guide target. We use moderate atomic number materials solid of low density foam aluminium as the wire-guide and solid density CH (plastic) as the substrate. This is the first time that foam is employed as a wire-guide material in these schemes. Low density porous materials (foam) becomes attractive in laser-plasma interactions for their unique properties. Compared to the solid, foams are less

collisional, can be heated volumetric (temperature and density are relatively uniform) and their resistivity more relevant to the FI scheme[24,25]. Foams have been used in laser-plasma interactions, for example, to smooth the laser energy deposition onto the ICF-target shell[26] and to study the fundamental plasma processes related to high energy density physics[27]. We found by using foam in those guides that fast electrons can penetrate to depths greater than observed in a pure solid density guide.

We studied the magnetic collimation dynamics in resistive guide targets with foam elements, and we have compared this to resistive guide targets composed only of solid density elements. It is known that, for moderate-Z solids, resistively-generated electric and magnetic fields dominate over collisional drag and scattering. Since these fields are resistively generated, excellent knowledge of material resistivity is required especially in the temperature range of $1-$ 100 eV, i.e. warm dense matter regime[28,29], as this temperature regime determines the nature of the resulting collimation and transport of the fast electrons. One of the key parameters in describing resistivity across the low temperature regime is the minimum mean free path. The maximum resistivity is expected to occurs when the minimum electron mean free path limits the electron collision frequency. In turn the minimum mean free path should be limited by the interatomic spacing, r_s, which is a function in ion density, i.e. $r_s = (3/4\pi n_i)^{1/3}$. The foams in this numerical study are defined from the reduction of ion density compared to that in the equivalent solid. The resistivity is independent of ion density in Spitzer regime, where the plasma is fully ionised and has temperature range of keV (assuming Z is not very high). Thus, the resistivity of both foam and solid would be similar in this regime. In the case of low-temperature regime, the situation is totally different as the value of the minimum mean free path should define the resistivity within the guide, especially in hybrid target materials like our targets. We found that the collimation dynamics are affected by the absolute value of the minimum mean free path close to injection region. Therefore we explored the effect of changing this parameter on the magnetic collimation. The present analysis underscores that long mean free path is preferable for an excellent collimation in foams. Finally we show that the advantages of each solid guide and foam guide can be combined into one guide under certain construction conditions.

It is worth mentioning that this study is limited to warn dense matter regime with a minimum temperature is 1 eV. This enables the use of the computationally efficient Lee-More resistivity model[30]. This includes electron degeneracy and screening effects, which are characteristic

of high density relatively cool plasmas. The model, and this work, does not attempt to describe plasmas at lower temperatures lattice structure effects discussed by Benuzzi et al.[31] or the density functional quantum molecular dynamics approach[32].

II. THE THEORY OF FOAM GUIDE'S MAGNETIC COLLIMATION

Finite plasma resistivity leads to the generation of significant magnetic fields when electron beams propagate through dense plasma, particularly when a resistivity gradient or shear in the fast electron current density exists. The magnetic field growth rate is given by[33],

$$\frac{\partial \vec{B}}{\partial t} = \eta(\nabla \times \vec{j}_f) + (\nabla\eta) \times \vec{j}_f \tag{1}$$

where η is the resistivity and $\vec{j}_f$ is the fast electron current density. The first term on the right hand side acts to concentrate the fast electrons to higher current density region, while the second term will guide the fast electrons towards higher resistivity region. In the context of the resistive guide[16] targets, the dynamics of collimation are as follows: $(\nabla\eta) \times \vec{j}_f$ term initiates the collimation at the early stage of the interaction since resistivity gradients are present by construction. Consequently, significant numbers of the fast electrons will be concentrated in the high resistivity region (the guide element) with some shearing, i.e. $\eta(\nabla \times \vec{j}_f)$. The latter term reinforces the collimated magnetic field, prolonging the collimating effect. Thus choice of the guide and substrate materials are critical in ensuring that the resistive guide functions properly. In this work, we studied this process using a foam wire-guide element that was embedded within a solid substrate. We used a choice of laser parameters that resulted in good quality fast electron collimation with a solid wire-guide element in a solid substrate[19], in order to compare the performance of the foam guide against a high quality reference case.

Plots of solid and foam resistivities of the materials used in this work over a temperature range of 0.1 to 1 keV are shown in Figure 1.These plots are generated using Lee-More resistivity model[30]. At high temperature, there is no significant difference in resistivity between foam and solid materials, as the materials should approach the Spitzer resistivity. So in terms of magnetic collimation both materials will exhibit similar behaviour. The low temperature regime is a different matter. At temperatures which are still low (1–10 eV), the foam resistivity is higher than the solid resistivity. This implies that the foam wire-guide

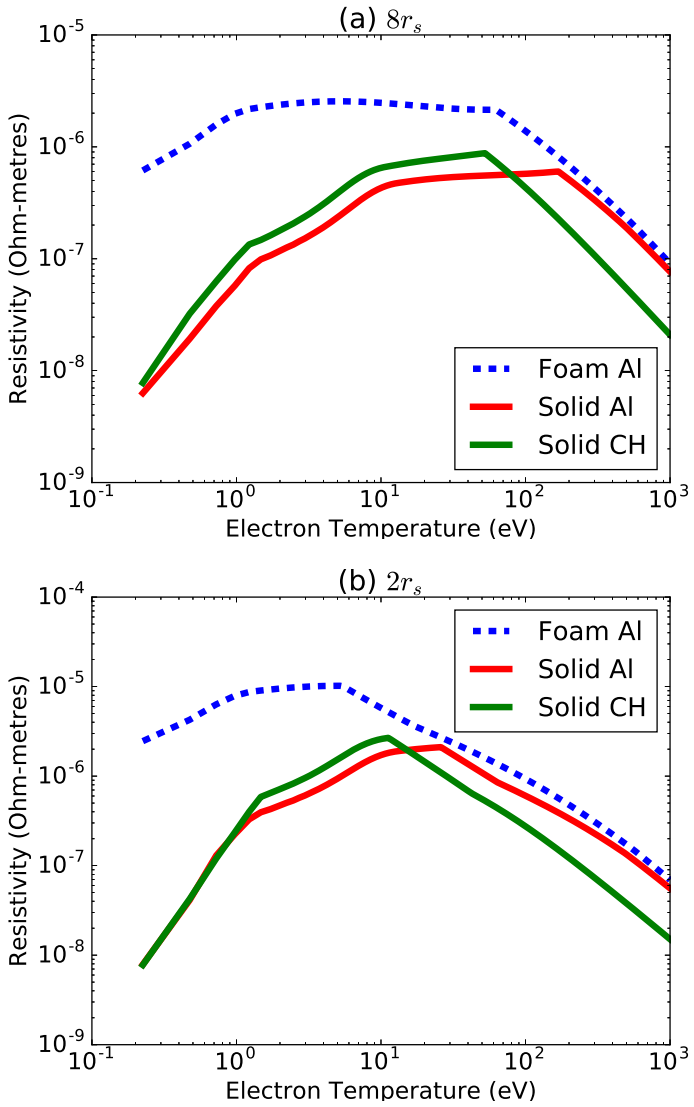

Figure 1: Plots of the resistivity at solid (sold lines) aluminium and plastic and an aluminium foam (dashed lines) at 10% solid density over a temperature range of 0.1 to 1 keV for materials used in this work; two different values of the minimum m.f.p. are investigated, (a) $8r_s$ and (b) $2r_s$, where r_s is the interatomic spacing.

acts a resistivity-gradient-driven guide when it is surrounded by a lower resistivity solid substrate. The difference between foam and solid resistivity at this regime depends on the absolute value of the minimum mean free path (m.f.p.) for the electrons. Two different values of the m.f.p. are investigated, $8r_s$ (Figure 1(a)) and $2r_s$ (Figure 1(b)), to study the effect of changing this parameter on the growth of collimating magnetic field. They both are linked by the fact that the m.f.p governs collisions of the background electrons. When a long

m.f.p is set the background electrons become less collision and their mobility increases. This helps to provide more return current to balance the fast electrons in order to generate resistive magnetic field. As shown in Figure 1(a), the difference between the two resistivities in low temperature regime is large, and when the value of m.f.p. is $8r_s$ these differences remain large for temperatures that exceed 10 eV. Using a foam wire-guide element is a possibility that ought to be considered, as it should allow for higher resistivities at low temperatures, which might result in a better performing guide.

It should be noted that, in the case of a foam wire-guide element, there may be issues with the growth of the de-collimating magnetic field close to the injection region. This de-collimating field grows along a certain length of the foam wire-guide element, and then beyond this length a collimating field strongly grows. The de-collimating field develops due the resistivity gradient being reversed in the strongly heated region close to the fast electron injection zone. This acts to expel fast electrons from the guide. The choice of the m.f.p. value changes the longitudinal extent of de-collimating magnetic field. We found that a long m.f.p. suppresses de-collimating field length which implies more fast electrons confined within the foam wire-guide. When the minimum m.f.p. is $8r_s$, Figure 1(a), the resistivity of Al foam peaks at a temperature comparable to the peak in solid CH, i.e. at nearly 70 eV. Lower than this temperature, the difference between the two curves diverges. In contrast, there is a difference in the peak positions of approximately 6 eV at at lower temperatures of a few eV's when the minimum m.f.p. is $2r_s$, Figure 2(b). In this case, the de-collimating field longitudinal extent grows to longer distance which reduces the number of confined fast electrons within the wire-guide.

In spite of this problem of the low temperature resistivity, the magnetic field's sign are correctly switched into collimation phase over a certain distance. This is due to a longitudinal heating gradient in foam guide keeps the guide in higher resistivity compared to that of solid substrate. Thus the fast electrons are collimated due to a relatively long pulse duration and the shear in the fast electron current density inside the wire, $\eta(\nabla \times \vec{j}_f)$. Once this takes place, the fast electrons transport to greater depth than that observed in solid guide, this is due to a reduction of background electron collisionality in the foam.

III. SIMULATIONS

A. Set-up

To draw a robust comparison of the magnetic collimation and of fast electron transport between foam and solid guides, we used a specific set of laser parameters that provided good quality fast electron transport in solid guides (See Ref[19] for further details). Simulations carried out by using the three-dimensional particle-in-cell (PIC) hybrid ZEPHYROS code[4]. The simulation parameters were set up as follows: a $400 \times 200 \times 200$ μm^3 grid was used with a 1 μm cell size in the x-direction and a 0.5 μm cell size in the y- and z-directions. The number of macroparticles injected into each cell within the focal spot was 124 which provided fair resolution. The targets consisted of CH (plastic) solid substrate, Z=3.5 and $n_i = 9.2 \times 10^{28}$ m^{-3}, within which a 5 μm wire (guide) radius was embedded and made co-linear with the x-axis and is centred on $y = z = 50$ μm. The type of wire-guide material used in each simulation is tabulated in Table I alongside with the choice of the absolute minimum mean free path (m.f.p.). The background resistivity uses model depicted in Figure 1 which closely follows the Lee and More description. The background temperature is initially set to 1 eV everywhere. The background fluid equation and the ionsiation degree were calculated using Thomas-Fermi model. The laser irradiation intensity was $5 \times 10^{19}\,\mathrm{W\,cm^{-2}}$ at a wavelength of λ_L =0.5 µm, with the assumption that 30% of the energy is coupled to a fast electron population. The fast electron temperature was set according to the Wilks' ponderomotive scaling[34],

$$T_{pond} = 0.511 \left[\sqrt{1 + \frac{I_L \lambda_L^2}{1.38 \times 10^{18}\ \mathrm{Wcm^{-2}}}} - 1 \right]\ \mathrm{MeV} \tag{2}$$

The temporal profile of the injected fast electron beam is a top-hat shaped with a pulse duration of 1 ps. The focal spot radius, r_{spot}, is 5 μm with intensity profile $\propto \exp[-\frac{r^2}{2r_{spot}^2}]$. The fast electron angular distribution is uniform over a divergence half-angle θ_d of 30°. The fast electron beam is injected into each target centred at the wire-guide centre. A total of six simulations were carried out and they are labelled A-F. Simulations A-D use a pure Al solid or Al foam wire as guide with varying the m.f.p. values as shown in Table 1. Simulations E and F use a wire that is made of solid up to a certain distance then it is made of foam and this has been tested with two different m.f.p. values. Notice that foam in our work is simply the low-density porous materials that is 10% of its solid density, i.e. for Al foam

n_i =6.127 m^{-3} and ρ =275 $\mathrm{kg\,m}^{-3}$ (0.275 $\mathrm{g\,cm}^{-3}$). We did not take in our account the pore size, its distribution and whether the cell structure is open or closed.

Simulation	wire-guide material	Min m.f.p.
A	Al solid	$8r_s$
B	Al foam	$8r_s$
C	Al solid	$2r_s$
D	Al foam	$2r_s$
E	Al solid then Al foam	$8r_s$
F	Al solid then Al foam	$2r_s$

Table I: Table of wire-guide materials and minimum mean free path (m.f.p.) in each simulation. The foam density is 10% of solid density, and r_s is the interatomic spacing.

B. Results

As stated above, the simulation setting up was chosen to provide an excellent magnetic collimation and fast electron transport[19]. The resulting collimating magnetic field, at 1.5 ps, and fast electron density, at 1 ps, are shown in Figures 2(a,b) for solid guide, simulation A, alongside foam guide, simulation B. The azimuthal magnetic field is generated along the x-direction at the interface between the wire and its substrate, i.e. at the region where the resistivity gradient exists, which in our simulations at $45 \leq y \leq 55$ µm. In these plots, the laser strikes centrally on the left hand boundary. For solid guide case, simulation A, the collimating field grows up to nearly $x = 200$ µm while in foam guide, simulation B, it grows up to the end of the simulation box, 400 µm. The reason for stopping the field growth in A, before $x = 200$ µm, is that beyond this distance the resistivity gradient condition for a collimating magnetic field does not apply. In this region, for solids, the temperatures are too low, Figure 1(a). In simulation A the temperature of the solid wire drops to nearly 50 eV at $x = 200$ µm. This is where the CH substrate resistivity is greater than the resistivity of the Al solid wire-guide. In addition, the longitudinal decline in the fast electron density in solid wire-guide, due to scattering and collisions, prevents the generation of the resistive

magnetic field. Thus, both reasons cause fast electrons to escape from the solid wire-guide. Yet in simulation B, the Al foam resistivity is greater than that of CH solid over large range of temperatures, Figure 1(b). This aids the collimating magnetic field to extend to longer longitudinal distances.

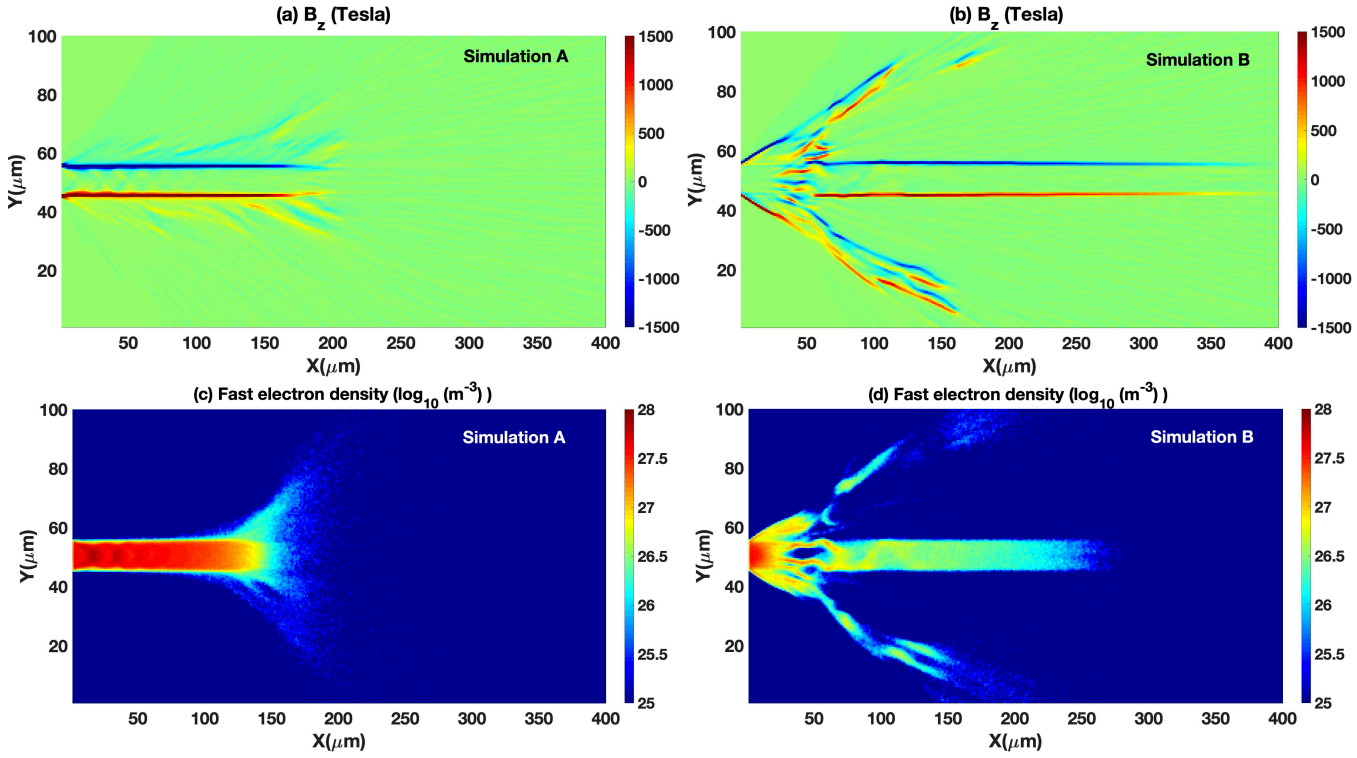

Figure 2: (a) and (b) the magnetic flux density, $B_z(T)$, at 1.5 ps and (c) and (d) logarithmic scale of the fast electron density, at 1 ps, for simulations A and B, respectively. The m.p.f. value is $8r_s$.

The extended field in B enhances a long propagation and confinement for the fast electrons within the guide. This is shown in Figure 2(d) as the fast electrons travel along the guide up to 250 μm at the end of the laser pulse which is longer than that in A at this particular time, Figure 2(c), by 100 μm. However, the fast electron number density is higher in A than in B. This is due to the growth of de-collimating magnetic field in B close to the injection region. This drives some of the fast electrons out the foam wire-guide.

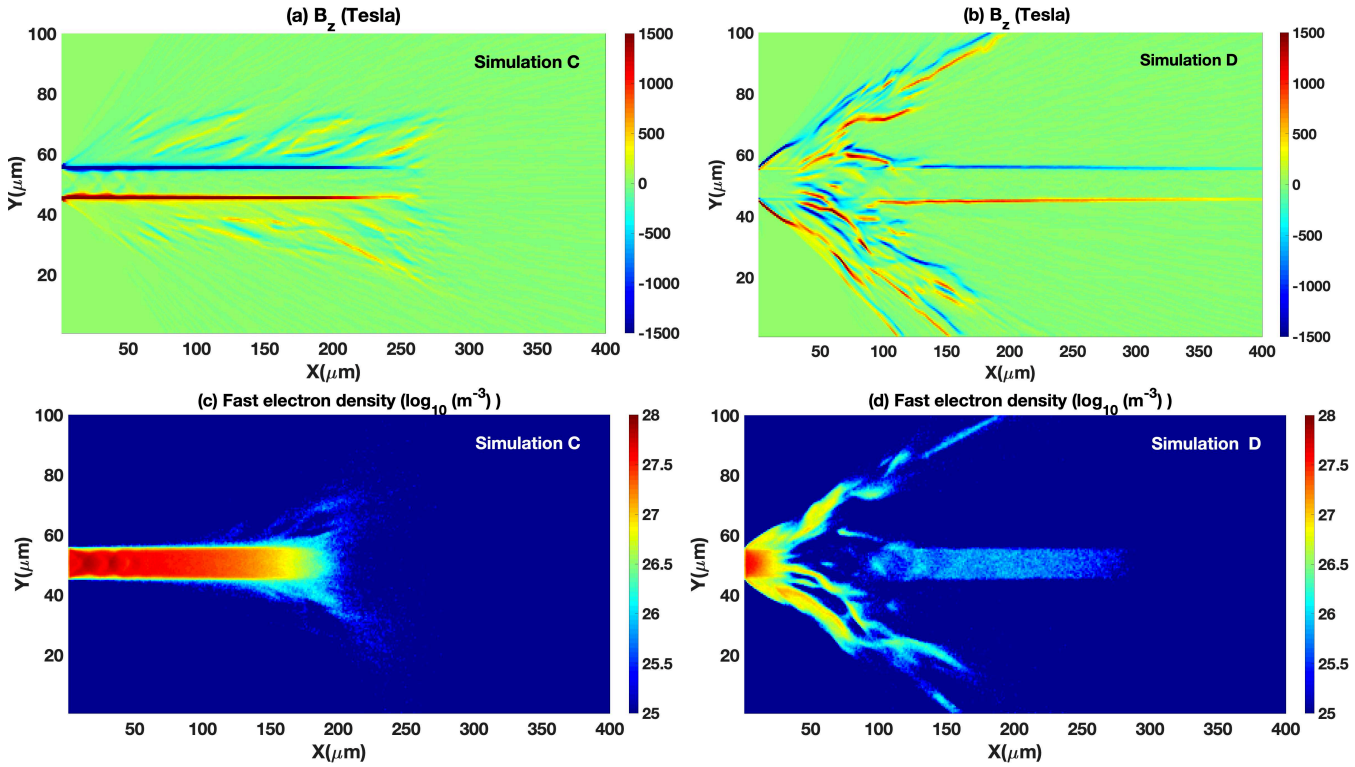

Figure 3: (a) and (b) the magnetic flux density, $B_z(T)$, at 1.5 ps and (c) and (d) logarithmic scale of the fast electron density, at 1 ps, for simulations C and D, respectively.The m.p.f. value is $2r_s$.

The de-collimating magnetic field is mainly affected by the low temperature cold-electron m.f.p. To study this effect, we repeat simulations A and B by setting cold-electron m.f.p. to $2r_s$, instead of $8r_s$. These are simulations C and D and the resulting magnetic field is shown in Figure 3. For solid guide, simulation C, the field grows up to $x = 250$ μm which is 50 μm longer compared to A which implies longer tolerance for resistivity gradient condition. This can be seen from Figure 1(b) as the values of the two solid density resistivites, for Al and CH, start to reverse below 1 eV. The fast electrons in Figure 3(c) travel for longer compared to that in simulation A for equivalent times in the simulations. In foam guide, simulation D, the collimating field grows up to the end of the simulation box as in B but a much lower number of the fast electrons are confined within the wire-guide, shown in Figure 3(d), due

to longer de-collimating field compared to that of B. We can conclude from simulations B and D that longer m.f.p. is needed in foam guides for better magnetic collimation. When the m.f.p. is long enough the difference in resistivity between foam guide and solid substrate becomes significant at temperatures below few 10's eV (Figure 1(a)). So this limits the range of temperature where the de-collimating field grows, i.e. the field only occurs at temperature above 100 eV. In the case of short m.f.p. this temperature range is extended from 1 eV to 1 keV, Figure 1(b), which means that de-collimating field would persist for longer.

We can see from simulations A-D that each wire-guide has its advantage; the solid wire-guide can confined higher fast electron number density while in a lower density foam wire-guide the fast electrons can travel to great depth. One might question how to combine advantages from both guides into one guide. Figure 4(a) shows the suggested construction of a wire-guide that could confine large numbers of fast electrons with long travel through the guide. Here, the wire-guide's material is longitudinally changes from solid on the left to foam on the right. The laser centrally strikes on the solid wire-guide at the left hand boundary to avoid the de-collimating field growth. In addition, the length of solid part of the wire-guide is shorter than the length where the magnetic collimation stops. In our test of this new configuration, we used the length observed from simulation A, i.e. solid material is up to $x = 150\,\mu\text{m}$. This is simulation E and the resulting fast electron density line-out is compared to simulations A and B in Figure 4(b). Notice that m.f.p. is set to $8r_s$ in these simulations. As shown, simulation E confines large numbers of fast electrons that are able to travel up to $x = 300\,\mu\text{m}$ at 1.5 ps. This is better outcome than for both simulations A and B. At $50 \leq x \leq 150$ μm, the fast electrons density of simulations A and E are identical since this is the region where both wire-guides are solid. Beyond this region, the fast electron number density gradually drops in A due to the lack of the magnetic collimation. This behaviour is noted in E but the drop in the fast electrons is steep at the transition region from solid to foam, yet quickly recovers to a fast electrons number density of $10^{27}\,\text{m}^{-3}$ then starts to drop gradually with increasing distance along x. Finally simulation B, pure foam wire-guide, shows the longest longitudinal travel, i.e. along x, of the fast electrons although number density is modest compared to values obtained in simulations A and E.

For simulation E, the observation of a sudden drop in fast electron number density is due to some limited growth of a de-collimating magnetic field at the transition region. This is shown in Figure 5(a). The emergence of a de-collimating field, which extends for 10 µm along

x, is followed by a fast growth in a collimating field. Figure 5(a) also shows the development of a strong and highly disruptive magnetic field in the foam wire-guide. This interior fields affects the fast electron transport in foam region of the wire-guide as shown in Figure 5(c), which degrades the magnetic collimation up to the end of the simulation box, i.e. x =400 µm. The interior magnetic field in simulation E is driven by inhomogeneous transport of the fast electrons. This results from the divergent flow of electrons and the gradient in the fast electron density as the electrons emerge from the solid wire-guide and couple to the foam wire-guide. In contrast, no such field has developed in the case of simulation F, the has the same guide structure but with reduced m.f.p. of $2r_s$, Figure 5(b). Here the length of de-collimating field is long compared to that of simulation E, this enables more fast electrons to escape from the wire-guide. Notice that Figures 5(c) and (d) show the fast electron number density 0.3 ps earlier at 1.2 ps to more clearly illustrate the transport of the fast electrons between solid and foam regions of the wire-guide.

IV. CONCLUSION

The magnetic collimation of fast electrons and their transport in foam guides have been investigated using laser parameters that resulted in good propagation through the solid guide (for the purpose of comparison). Numerical calculations carried out using three dimensional hybrid PIC code ZEPHYROS showed that the fast electron penetration in the foam guide is much greater than in the solid guide. Importantly, we showed that foam guide still works even when there is substantial de-collimating field growth near the injection region, as the collimating field extended to the end of the simulation box. The numerical work also showed that a combined solid-foam wire-guide, or hybrid resistive guide target, is able to combine the benefit of both pure solid and pure foam guides; large number of the fast electrons can travel deep through the wire.

By using moderate-Z materials (aluminium and plastic) we ensure full ionisation and Spitzer resistivity holds for moderate temperatures, above 100 eV. The resistivity acts on the cooler background electrons, not the injected fast electrons. At lower temperatures, 10 eV or so and below, the resistivity depends upon the density and significantly increases with a foam, potentially creating a better resistive guide. We find with a foam, close to the fast electron injection region, a low heat capacity results in strong heating with the formation of a de-

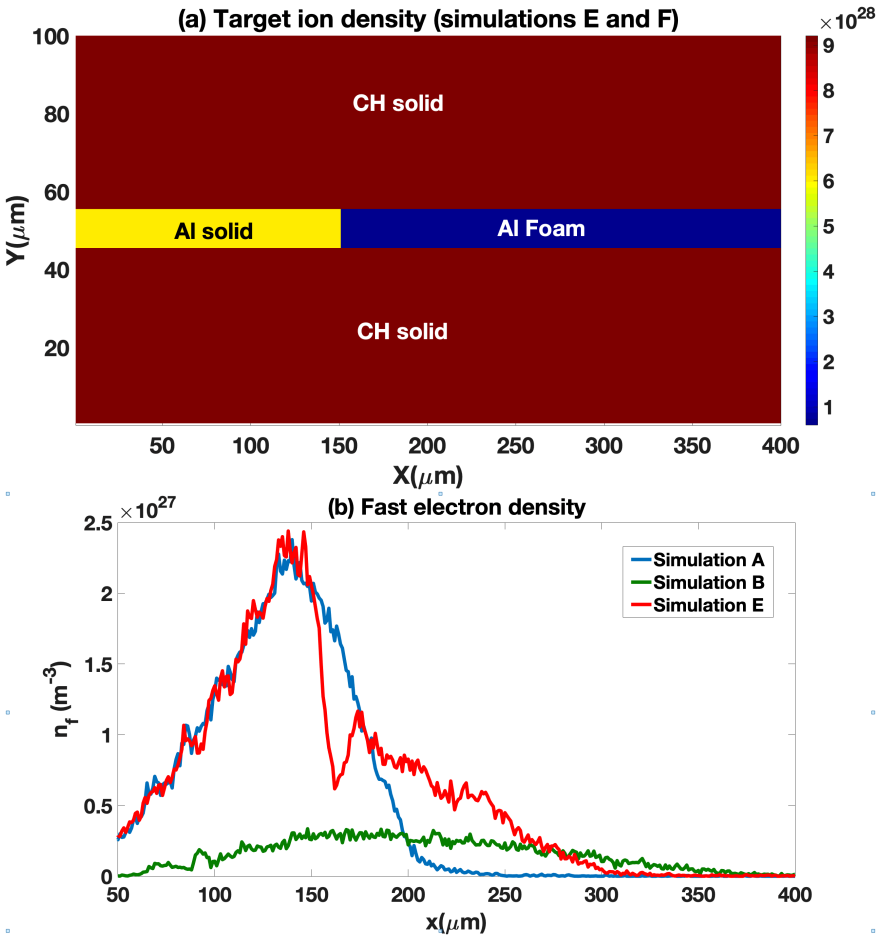

Figure 4: (a) Target ion density profile for simulations E and F. (b) Line-out of the fast electron density (m^{-3}) at 1.5 ps from simulations A, B and E. The m.p.f. is $8r_s$ in these simulations.

collimating field and an associated loss of fast electrons. Further along the wire-guide, the temperature drops and a rapidly growing now collimating field forms, this enables the remaining fast electrons in the wire-guide to take advantage of the low density and reduced collisionality to propagate the entire length of the guide. Our hybrid resistive guide target, uses the excellent collimating properties of a solid density wire-guide at the injection site, and at appropriate distances from this region, couples these electrons to a low collisionality foam wire-guide for an excellent collimation in the foam.

It is possible that the effective guiding demonstrated here can be employed in applications of fast electron transport. Fast ignition inertial confinement fusion is a possibility, but a more proximate application is likely to be the generation of warm or hot dense matter.

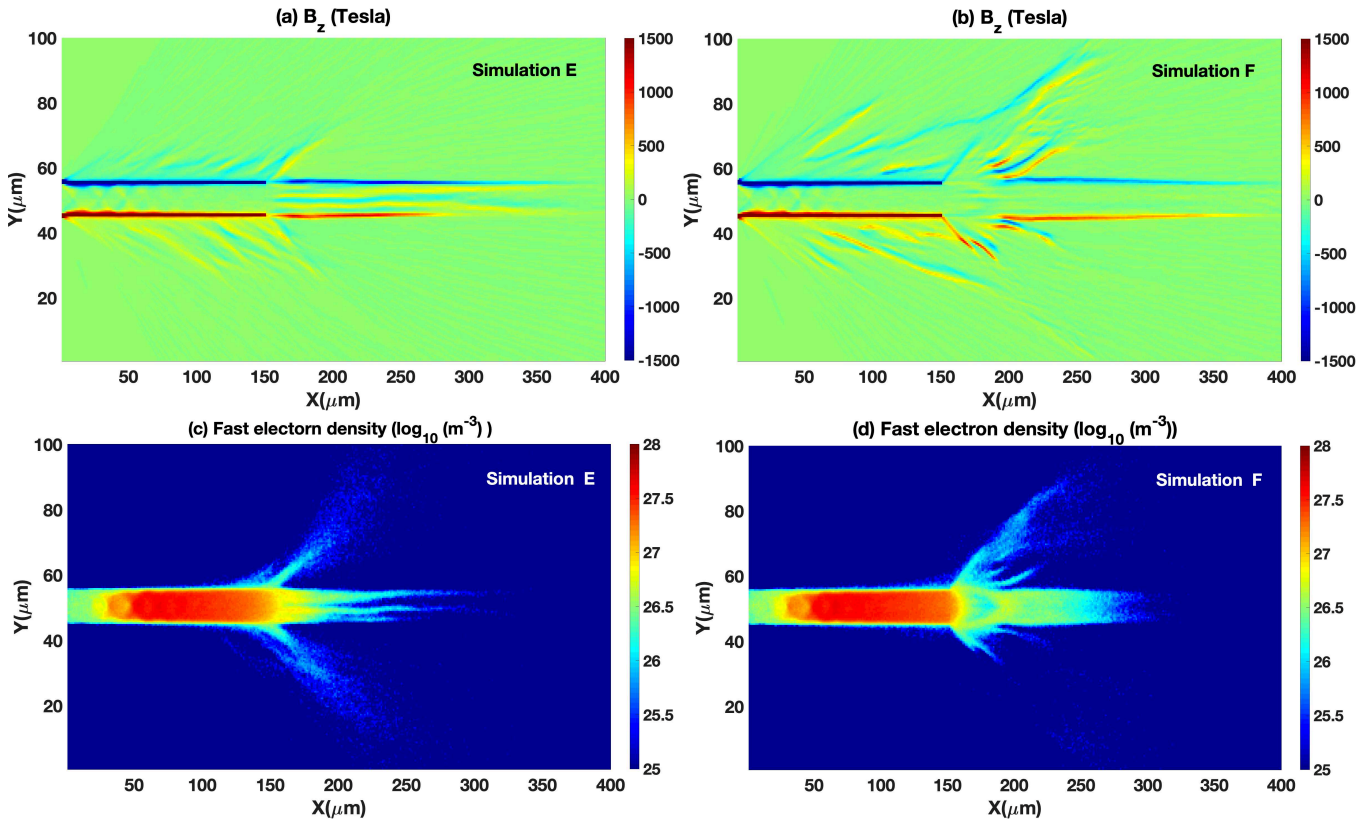

Figure 5: (a) and (b) the magnetic flux density, $B_z(T)$, at 1.5 ps and (c) and (d) the fast number electron density at 1.2 ps, for simulations E and F, respectively and plotted using logarithmic colour scale.

V. ACKNOWLEDGMENTS

The authors are grateful for the use of computing resources provided by STFC's Scientific Computing Department. The author (RABA) was supported by a grant from the "Research Center of the Female Scientific and Medical Colleges", Deanship of Scientific Research, King Saud University. APLR is grateful for support from the ERC via STRUCMAGFAST grant (ERC-STG-2012). All data used to produce the figures in this work, along with any other supporting material, can be found at http://dx.doi.org/10.15124/7353ade9-3428-4f5a-a837-cb3532e4193f.

REFERENCES

[1]K. L. Lancaster, J. S. Green, D. S. Hey, K. U. Akli, J. R. Davies, R. J. Clarke, R. R. Freeman, H. Habara, M. H. Key, R. Kodama, et al., Phys. Rev. Lett. **98**, 125002 (2007).

[2]J. S. Green, V. M. Ovchinnikov, R. G. Evans, K. U. Akli, H. Azechi, F. N. Beg, C. Bellei, R. R. Freeman, H. Habara, R. Heathcote, et al., Phys. Rev. Lett. **100**, 015003 (2008).

[3]R. Freeman, D. Batani, S. Baton, M. Key, and R. Stephens, Fusion science and technology **49**, 297 (2006).

[4]A. P. L. Robinson, D. J. Strozzi, J. R. Davies, L. Gremillet, J. J. Honrubia, T. Johzaki, R. J. Kingham, M. Sherlock, and A. A. Solodov, Nuclear Fusion **54**, 054003 (2014).

[5]R. G. Evans, Plasma Phys. Control. Fusion **49**, B87 (2007).

[6]D. Strozzi, M. Tabak, D. Larson, L. Divol, A. Kemp, C. Bellei, M. Marinak, and M. Key, Phys. Plasmas **19**, 072711 (2012).

[7]M. Tabak, J. Hammer, M. E. Glinsky, W. L. Kruer, S. C. Wilks, J. Woodworth, E. M. Campbell, M. D. Perry, and R. J. Mason, Phys.Plasmas **1**, 1626 (1994).

[8]A. R. Bell and R. J. Kingham, Phys. Rev. Lett. **91**, 035003 (2003).

[9]S. Bolaños, J. Béard, G. Revet, S. Chen, S. Pikuz, E. Filippov, M. Safronova, M. Cerchez, O. Willi, M. Starodubtsev, et al., Matter and Radiation at Extremes **4**, 044401 (2019).

[10]M. Bailly-Grandvaux, J. Santos, C. Bellei, P. Forestier-Colleoni, S. Fujioka, L. Giuffrida, J. Honrubia, D. Batani, R. Bouillaud, M. Chevrot, et al., Nature communications **9**, 102 (2018).

[11]H. Xu, X. Yang, J. Liu, and M. Borghesi, Plasma Phys. Control. Fusion **61**, 025010 (2019).

[12]X. Yang, M. Borghesi, and A. Robinson, Phys. Plasmas **19**, 062702 (2012).

[13]A. P. L. Robinson, M. Sherlock, and P. A. Norreys, Phys. Rev. Lett. **100**, 025002 (2008).

[14]R. H. H. Scott, C. Beaucourt, H.-P. Schlenvoigt, K. Markey, K. L. Lancaster, C. P. Ridgers, C. M. Brenner, J. Pasley, R. J. Gray, I. O. Musgrave, et al., Phys. Rev. Lett. **109**, 015001 (2012).

[15]S. Malko, X. Vaisseau, F. Perez, D. Batani, A. Curcio, M. Ehret, J. Honrubia, K. Jakubowska, A. Morace, J. J. Santos, et al., Scientific reports **9**, 1 (2019).

[16]A. P. L. Robinson and M. Sherlock, Phys. Plasmas **14**, 083105 (2007).

[17]S. Kar, A. P. L. Robinson, D. C. Carroll, O. Lundh, K. Markey, P. McKenna, P. Norreys, and M. Zepf, Phys. Rev. Lett. **102**, 055001 (2009).

[18]B. Ramakrishna, S. Kar, A. P. L. Robinson, D. J. Adams, K. Markey, M. N. Quinn, X. H. Yuan, P. McKenna, K. Lancaster, J. Green, et al., Phys. Rev. Lett. **105**, 135001 (2010).

[19]A. P. L. Robinson, H. Schmitz, and J. Pasley, Phys. Plasmas **20**, 122701 (2013).

[20]R. A. B. Alraddadi, A. P. L. Robinson, N. C. Woolsey, and J. Pasley, Phys. Plasmas **23**, 072706 (2016).

[21]A. P. L. Robinson, H. Schmitz, J. S. Green, C. P. Ridgers, N. Booth, and J. Pasley, Phys. Plasmas **22**, 043118 (2015).

[22]R. A. B. Alraddadi, A. P. L. Robinson, J. Pasley, and N. C. Woolsey, Phys. Plasmas **25**, 023104 (2018).

[23]A. P. L. Robinson, H. Schmitz, J. S. Green, C. P. Ridgers, and N. Booth, Plasma Phys. Control. Fusion **57**, 064004 (2015).

[24]B. Ramakrishna, P. Wilson, K. Quinn, L. Romagnani, M. Borghesi, A. Pipahl, O. Willi, L. Lancia, J. Fuchs, R. Clarke, et al., Astrophysics and Space Science **322**, 161 (2009).

[25]K. Nagai, C. S. Musgrave, and W. Nazarov, Phys. Plasmas **25**, 030501 (2018).

[26]M. Dunne, M. Borghesi, A. Iwase, M. Jones, R. Taylor, O. Willi, R. Gibson, S. Goldman, J. Mack, and R. Watt, Phys. Rev. Lett. **75**, 3858 (1995).

[27]S. Chen, T. Iwawaki, K. Morita, P. Antici, S. Baton, F. Filippi, H. Habara, M. Nakatsutsumi, P. Nicolaï, W. Nazarov, et al., Scientific reports **6**, 21495 (2016).

[28]A. P. L. Robinson, H. Schmitz, and P. McKenna, New J. Phys. **17**, 083045 (2015).

[29]N. Booth, A. P. L. Robinson, P. Hakel, R. J. Clarke, R. J. Dance, D. Doria, L. A. Gizzi, G. Gregori, P. Koester, L. Labate, et al., Nature communications **6**, 1 (2015).

[30]Y. T. Lee and R. M. More, Phys. Fluids **27**, 1273 (1984).

[31]A. Benuzzi, M. Koenig, B. Faral, J. Krishnan, F. Pisani, D. Batani, S. Bossi, D. Beretta, T. Hall, S. Ellwi, et al., Phys. Plasmas **5**, 2410 (1998).

[32]T. White, S. Richardson, B. Crowley, L. Pattison, J. Harris, and G. Gregori, Phy. REv. Lett. **111**, 175002 (2013).

[33]A. R. Bell, J. R. Davies, and S. M. Guerin, Phys. Rev. E **58**, 2471 (1998).

[34]S. C. Wilks, W. L. Kruer, M. Tabak, and A. B. Langdon, Phys. Rev. Lett. **69**, 1383 (1992).